Extended Abstracts of the 2008 International Conference on Solid State Devices and Materials, Tsukuba, 2008, pp. 1070-1071

H-7-3

High-frequency capacitance measurements in GaAs/AlGaAs quantum dots

Takeshi Ota, Toshiaki Hayashi, and Toshimasa Fujisawa

NTT Basic Research Laboratories, NTT Corporation, 3-1, Morinosato Wakamiya, Atsugi, 243-0198, Japan

1. Introduction

The charge-sensors with fast operation and high sensitivity are promising tools for single-shot readout of electronic states in the quantum information processing. For this purpose, mesoscopic-scale devices such as a single-electron transistor (SET) and a quantum point contact (QPC), integrated in a radio-frequency impedance matched circuit, have been employed to detect charge configurations in quantum dots [1]. The derivative of the charge with respective to the applied gate voltage, $C = dQ/dV_G$, which can be regarded as a capacitance, is a complementary quantity to the charge in the sense that it can measure the tunneling coupling of a double quantum dot (DQD) [2]. However, capacitance measurements are usually restricted to low-frequency regime, since numerical derivation or room-temperature electronics are used.

In this work, we demonstrate novel high-frequency capacitance measurements in an electrostatically-defined DQD coupled to a QPC. By employing on-chip Lock-in technique with two RF signals, the operating frequency ν_{op} can be increased up to the order of a few tens GHz. We confirm the high-speed capacitance measurement by ν_{op} dependence and phase analysis. Using this technique, we estimate the time constants of the tunneling barrier, which depends on the electron number in the dot.

2. Capacitance measurement

A DQD is formed in a two-dimensional electron gas in a GaAs/AlGaAs heterostructure by applying negative voltages to the surface Schottky metal gates. Figure 1(a) shows a schematic diagram of the experimental setup. The device is mounted in a dilution refrigerator with 130 mK of an electron temperature.

A QPC attached nearby to the DQD usually monitors the charge states of the DQD by measuring the current I_{QPC} at a finite dc voltage $V_{sd\text{-}QPC}$ [3]. Here, we consider zero dc current at zero dc voltage ($V_{sd\text{-}QPC} = 0$) for the capacitance measurements. The phase-tunable high frequency voltages V_{DQD} and V_{QPC} operating at ν_{op} are applied to the DQD and the QPC independently, allowing the Lock-in measurement of the impedance (capacitance and conductance). Modulation of the dot potential with V_{DQD} influences the charge state of the DQD and induces charge ΔQ on the QPC. The conductance of the QPC in the tunneling regime changes in response to ΔQ. By applying V_{QPC} at the same frequency and phase, one can obtain an average current $\langle I_{QPC}\rangle$ proportional to $\Delta Q = C\Delta V_{DQD}$, serving a capacitance measurement. When the phase of V_{QPC} is set at 90 degrees, $\langle I_{QPC}\rangle$ is proportional to the conductance of the system.

For demonstrating the capacitance measurements, we focus on tunneling processes across the right barrier as shown in Fig. 1(b). The upper trace of Fig. 1(c) shows $\langle I_{QPC}\rangle$, taken by conventional charge detection measurement, at a dc bias voltage $V_{sd\text{-}DQD}$ = 0.5 mV as a function of the gate voltage V_{UR}. The current $\langle I_{QPC}\rangle$ jumps every time the number of the electrons N in the right quantum dot is changed, as evidenced by the saw-toothed curve (i). The capacitance measurement is carried out at zero dc voltage ($V_{sd\text{-}QPC} = 0$) but in the presence of the two RF signals. In this case, $\langle I_{QPC}\rangle$ shows peaks instead of the jumps as shown in the lower trace (ii) of Fig. 1(c), indicating the increase of the capacitance at the charge

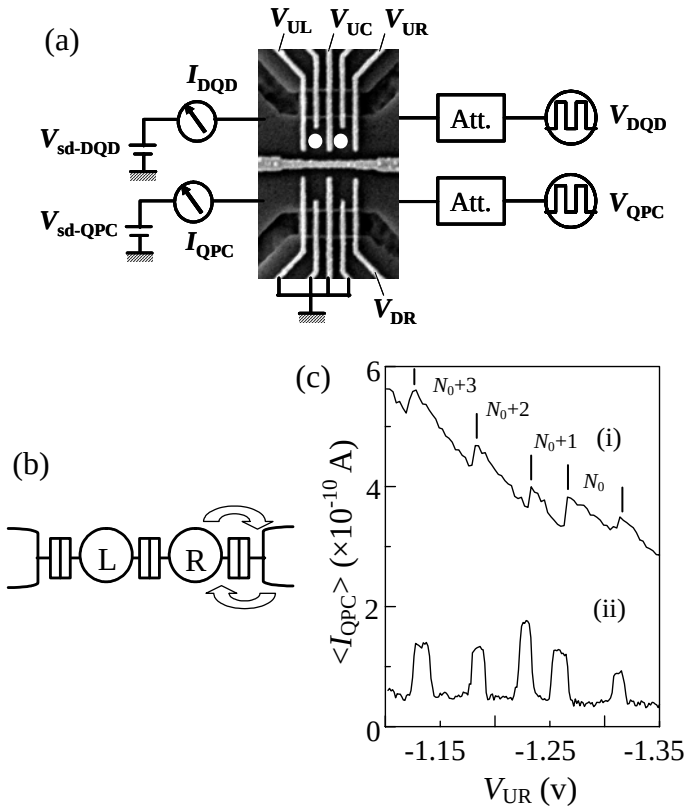

Figure 1 (a) Schematic diagram of the measurement setup. The sample shown in the SEM images contains a GaAs DQD indicated by the white circles. The upper and lower channel is electrically isolated. The right-end gate in the lower channel is used for the charge detection of the DQD. (b) Schematic diagram of the DQD. In this work, the electron number in the right dot is changed and that in the left dot is fixed. (c) The measured $\langle I_{QPC}\rangle$ as a function of the gate voltage V_{UR}. The curve (i) corresponds to $\langle I_{QPC}\rangle$ with applying DC voltages, i.e. 0.5 mV (0.7 mV) of $V_{sd\text{-}DQD}$ ($V_{sd\text{-}QPC}$). The curve (ii) indicates $\langle I_{QPC}\rangle$ taken by applying 0.4 mV (0.6 mV) of V_{DQD} (V_{QPC}) at ν_{op}=0.1 MHz. Here, $V_{sd\text{-}DQD}=V_{sd\text{-}QPC}=0$. N_0 corresponds to the number of the electrons in the right dot.

transition conditions.

The capacitance signal consists of two components as schematically shown in Fig. 2(c). The direct capacitive coupling between the QPC and the pulse electrode with V_{DQD} appears as a background (constant) signal δI_{CB}. The magnitude of this component should be given by the electrostatic geometry of the electrodes and the DQD. On the other hand, at the charge boundaries of the DQD, the peaks with amplitude δI_{peak} appear on the constant δI_{CB}. The tunneling process effectively short-circuits the two conductors, and thus the total capacitance is increased.

We analyze δI_{peak} and δI_{CB} as a function of the phase difference θ between the two RF voltages V_{DQD} and V_{QPC}, as shown in Fig. 2. Since the background signal δI_{CB} arises from the electrostatic effect, the characteristics should be independent of the frequency and is used as a reference. Actually, δI_{CB} becomes a maximum at $\theta = 0$ and minimum $\theta = 180$ degrees, showing same sinusoidal dependence on θ at all ν_{op}.

On the other hand, δI_{peak} shows similar sinusoidal dependence on θ, but the amplitude is decreased and phase is shifted as ν_{op} is increased [See arrows in Fig. 2(a)]. The impedance of the tunneling barrier can be expressed with a tunneling capacitance C_t and tunneling rate Γ_t. The amplitude of the peak is related to C_t, and the cut-off frequency is determined by Γ_t. Figure 3 shows the amplitude of δI_{peak} (capacitance) at $\theta = 0$ as a function of ν_{op}. The amplitude decreases with increasing ν_{op}. The data indicated by (i) to (iii) correspond to the peak amplitudes of N, N+1 and N+2 electron states, respectively. The solid lines are fitted using a simple model described in Ref. 3. From this fitting, the time constants of the tunneling barrier for N to N+2 states are estimated as Γ^{-1} = 0.4 nsec, 3 nsec and 20 nsec, respectively.

The maximum frequency for the capacitance measurement is more than 15 GHz (data not shown), which is practically limited by the quality of our low-temperature coaxial cables. The demonstrated high-frequency operation encourages single-shot capacitance measurement for electronic states in a DQD.

4. Conclusion

We have performed the high-frequency capacitance measurements in the quantum dots. This technique allows us to study spin/charge configurations in the double quantum dot, and possibly leads to future single-shot readout.

Acknowledgement

This work was supported by the SCOPE from the Ministry of Internal Affairs and Communications of Japan.

References

[1] L. DiCarlo, et al., Phys. Rev. Lett. 92, 226801 (2004).
[2] For example, R.J. Schoelkopf, et al., Science 280, 1238 (1998).
[3] T. Hayashi, et al., Jpn J. Appl. Phys. 45, 3629 (2006).

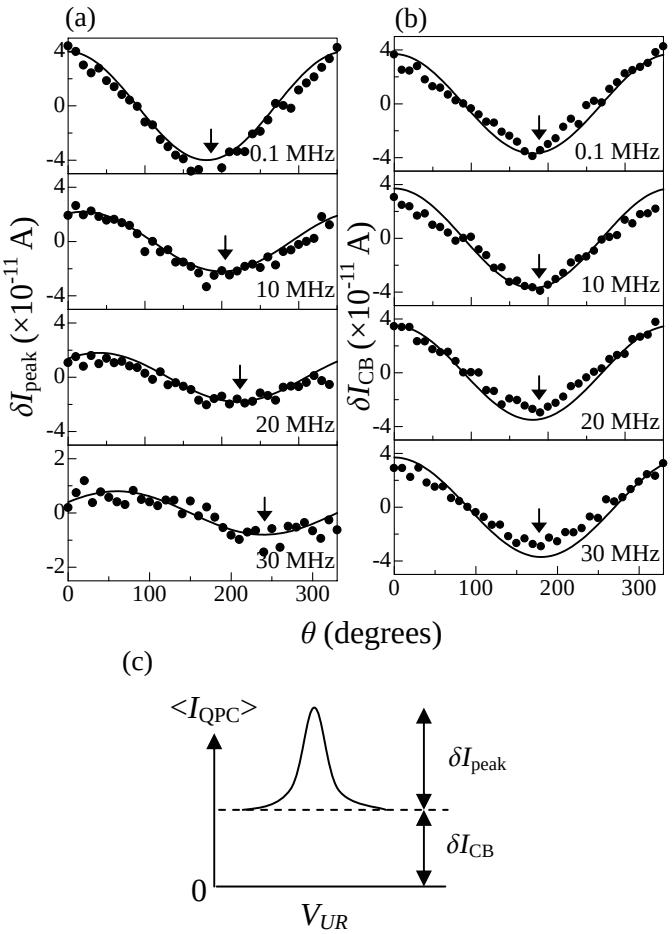

Figure 2 (a) δI_{peak} as a function of θ. (b) δI_{CB} as a function of θ. The solid lines in (a) and (b) are guide for eyes. The arrows show the positions of the dips. (c) Schematic illustration of the capacitance peak. The peak height δI_{peak} and the background signal δI_{CB} are defined as shown in the figure.

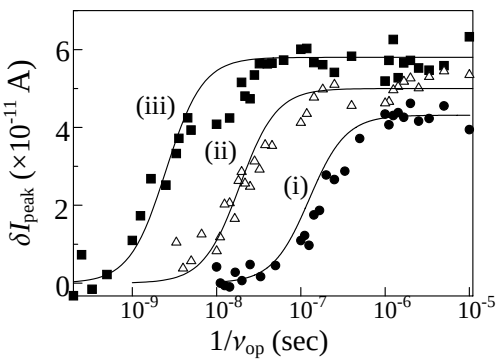

Figure 3 The amplitude of the in-plane components ($\theta = 0$) of δI_{peak} as a function of ν_{op}. The data indicated by (i) to (iii) correspond to the peak amplitudes of N, N+1 and N+2 electron states, respectively. Here, N is electron number in the right dot. The solid lines are fitted ones using a simple model.